Numerical Simulation of the Field and Frequency Limits for Volume coils in MRI

Bin Xu, Ian Gregg, Stuart Crozier and Feng Liu
School of Information Technology and Electrical Engineering,
University of Queensland, Brisbane, QLD 4072, Australia
Email: stuart@itee.uq.edu.au

Abstract

As signal to noise ratio in magnetic resonance imaging (MRI) improves with increasing static magnetic field strength there is a strong incentive to develop the technology to acquire images at higher fields. While magnet technology has made it possible to generate fields of 10 Tesla and more, limitations of the radio frequency (RF) hardware prevent the acquisition of high quality images over full regions of interest in clinical applications. Since its introduction, the birdcage coil [1] has become a very popular choice for volume imaging and this paper investigates the high frequency limits of several different sizes and designs of birdcage coils. Unloaded coils are simulated using commercial Method of Moments (MoM) software (FEKO [12]) and the capacitances and radii of the conductors are varied within practical limits to determine a maximum frequency of operation for each coil. Results show that practical birdcages are frequency limited to about 400 MHz for a typical head coil (27cm inside diameter, 30cm shield diameter and 25cm length); 128 MHz for a small whole body coil (60cm inside diameter, 64cm shield diameter and 70cm length) and 100 MHz for a large whole body coil (60cm inside diameter, 64cm shield diameter and 100 cm length). These limits are reduced when interactions with the load are taken into account and experience shows that a typical head coil is limited to about 200 MHz in practical experiments.

1. Introduction

Magnetic Resonant Imaging, known as MRI, is a powerful, non-invasive imaging technology that has played and will continue to play an important role in the Biomedical Imaging community. A key element in a MRI system is the radio-frequency (RF) coil, a resonant device used for transmitting and receiving electromagnetic energy at the Larmor frequency of a given nucleus of interest. The quality of the image depends upon the homogeneity of the RF magnetic field generated by the coil. The current generation of clinical MRI systems employ primary magnetic field intensities for human head at 3T, 4T, 7T and even 9T, and for the whole body MRI up to 4T [1, 2, 9 and 11] for which the Larmor frequencies are roughly 128 MHz, 174 MHz, 300 MHz and 400 MHz.

Today, nuclear MRI technologies are moving inexorably toward higher field strength in search of improved signal-to-noise ratio (SNR), spectral resolution and spatial resolution. As MRI moves to higher field and higher frequencies, the size of RF coils relative to the wavelength of operation becomes larger. The high magnetic field (frequency) technology has brought considerable challenges in engineering in the form of ancillary hardware, e.g., the radio frequency (RF) resonator [3, 4]. Current and past design procedures for RF coils, which have been quasi-static at lower frequencies, become inaccurate and full wave methods must be used. At higher frequencies wave-like phenomena become more important.

The birdcage coil was first developed by Hayes et al. for whole body NMR imaging at 1.5T [1,2]. While birdcage coils have been used very successfully at up to 200 MHz, their physical structure makes it impossible to them to operate in the same mode at higher frequencies. Higher resonant frequencies are achieved by reducing the inductance and capacitance of the components of the coil. However, a limit is reached where the conductors cannot be made larger and even without any lumped capacitors the stray capacity of the coil causes it to self resonate. As the stray capacity is not well controlled self resonant coils tend not to produce homogeneous field distributions.

As coils approach wave length dimensions, the performance of conventional lumped element designs and conventional birdcage coils encounter several problems [5] and do not achieve good performance. The transverse electromagnetic (TEM) resonator design [7, 8,and 9] has been proposed as a superior replacement for the standard birdcage coil in high-field applications. Some other volume coils such as cavity coils and re-entrant cavity (recav) coils have demonstrated better field homogeneity and a higher quality factor than an equivalent birdcage

coil at higher frequencies resulting in improved image quality [9, 11].

To obtain practical volume coils for clinical/experimental applications or design some novel coil types, however, it is still necessary to investigate the field and the frequency limits of conventional volume coil technology and here three different sized birdcage coils are simulated: a typical head coil (27cm inside diameter, 30cm shield diameter and 25cm length); a small whole body coil (60cm inside diameter, 64cm shield diameter and 70cm length) and a large whole body coil (60cm inside diameter, 64cm shield diameter and 100 cm length). The maximum frequency, field homogeneity and current distributions are determined for each to assist with selection of coils for higher frequency applications.

2. Theory and Methods

Analytic methods

A birdcage coil with N rungs has (N/2+1) modes and will resonate at (N/2+1) different frequencies. In these modes there is a dominant mode that produces the best B_1 field. In this dominant mode the currents on the rungs are sinusoidally distributed and hence the field closely approximates the homogeneous magnetostatic field produced by a sinusoidally distributed cylindrical surface current.

RF coils are usually made of conducting wires or conducting strips and discrete capacitors. At low frequencies where the size of the coil elements is small relative to the wavelength of the resonant frequency simple equivalent circuit models can be utilized [2]. The simplest equivalent circuit, ignoring mutual inductance, gives the following analytical solutions for the resonant frequencies for high pass and low pass birdcage coils:
For the high pass coil this is:

$$\omega_m = \left[C \left(L + 2M \sin^2 \left({}^{\pi m}/_{N} \right) \right) \right]^{-0.5} \tag{1}$$

and for the low pass birdcage coil it is:

$$\omega_m = \left[C \left(M + \frac{L}{2 \sin^2 \frac{\pi m}{N}} \right) \right]^{-0.5} \tag{2}$$

Where N is the number of rungs of the birdcage coil; M is the inductance of a rung of the coil, L is the inductance of each segment of the end ring, C is the capacitance on the rungs or end rings and m is the mode number.

Although these results are not very accurate they can be employed to examine the general effect of various parameters on the resonant frequencies. As the number of rungs is increased the resonant frequency of the dominant mode (m=1) of high pass coils will increase and the resonant frequency of low pass coils will decrease. To investigate the maximum frequency of operation the number of rungs should be chosen to be as large as is practical for the high pass coil and as low as practical for the low pass coil.

This method can be extended to take into account the mutual inductance between conductors and is highly efficient, reasonably accurate and thus very practical for low frequency cases. However, the analytic method does not provide accurate results for higher frequencies such as those investigated here where the length of the conductors become significant when compared to the wavelength.

Method of Moments (MoM)

A simulation approach based on method of moments (MoM) [2] as implemented by the commercial software package FEKO (EM Software & Systems) [12] is used here. This method does not require any assumptions regarding the current distribution on the conductors to be made. By providing a full wave solution of Maxwell's equations for both the currents and the fields it accurately models wavelength effects and coupling between conductors. It is very efficient for unloaded cases or cases where there is a simple, symmetrical load.

The simulation is set up as a conventional scattering problem where the unknown current distribution on the RF coil is solved by decomposing the problem into two parts. One is the impressed voltage source regarded as an incident electric field. Second is the scattered field due to an RF coil which functions as an object of scattering. [2]

A voltage source applied to the model is equivalent to an incident electrical field, E_i. To satisfy the boundary condition of zero tangential electrical field on the resonator conductors, the scattered field, E_s can be derived from

$$(\mathbf{E}_i + \mathbf{E}_s)\,|_{tangential} = 0 \tag{3}$$

The scattered field can be expressed as

$$\mathbf{E}_s(\mathbf{J}) = -jw\mathbf{A} - \nabla\Phi \tag{4}$$

where J is the current density induced on the surface of the objects, w is the operating frequency, A, Φ are the magnetic vector potential and electric scalar potential, respectively. These potentials can be expressed by using Green's functions G.

$$\begin{cases} \mathbf{A}(r) = \mu_0 \left(\iint_{S_1+S_2+S_3} \mathbf{J}(r')G(r,r')ds' \right) \\ \Phi(r) = \dfrac{-1}{jw\varepsilon_0} \left(\iint_{S_1+S_2+S_3} \nabla' \cdot \mathbf{J}(r')G(r,r')ds' \right) \end{cases} \tag{5}$$

Where S_1, S_2, S_3 denote the surfaces of the resonator, RF shield or cavity wall and head model, respectively.

In the MoM discretization the wires are divided into segments and the surfaces are divided into small triangular patches. The maximum dimension of these elements is chosen to be a small fraction, typically 1/10, of a wavelength at the highest frequency to be simulated. The currents on these elements are then decomposed into a linear combination of basis functions. After performing testing for each basis function, the integral equations are finally transformed into MoM matrix equations in the form of

$$[Z][I]=[V] \tag{6}$$

Where [Z] is the impedance matrix, [I] is the current to be determined and [V] is the voltage vector including the excitation source. The impedance matrix can incorporate terms representing lumped elements such as the capacitors in the birdcage coil. The impedance matrix is dense and hence equation (6) is solved using iterative techniques in conjunction with preconditioning.

Simulation parameters

Making the conductors thicker or using wide, thin strips minimizes the inductance and maximizes the resonant frequency as can be seen from the following formulae for self inductance:
For wire

$$L = 0.002l\left(\ln\frac{2l}{a}-1\right) \tag{7}$$

where l is the length and a is the radius of the wire.
For strips

$$L = 0.002l\left(\ln\frac{2l}{w}+\frac{1}{2}\right) \tag{8}$$

where l is the length of the strip and w is its width.
Here only wires are used in the simulation but combining (7) and (8) gives a simple conversion from wire radius to an equivalent strip width

$$w = 4.482\ a \tag{9}$$

Hence performing simulations with wire of different radii should be sufficient for the characterization of the maximum frequency of operation of these coils. For detailed design at the highest frequencies the differences between wires and strips should be taken into account.

Six different cases were simulated; both are high pass and low pass for each of the three sizes of coil. The high pass coils all have 16 rungs with lumped capacitors added to the centre of the rungs. The low pass coils all have 4 rungs with lumped capacitors added to the centre of each end ring segment. See Figure 1.

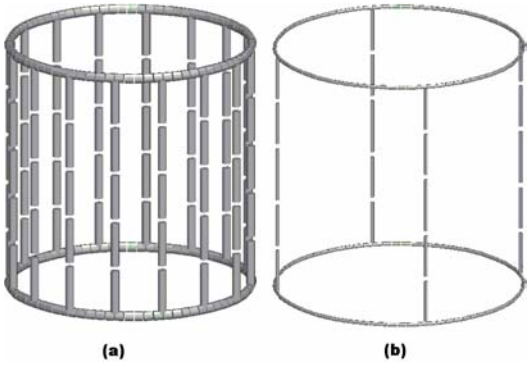

Figure 1 (a) 16 rung high pass birdcage coil
(b) 4 rung low pass birdcage coil
(The shield is not shown here)

Coils with wires of radius 0.5mm, 1mm, 2mm and 5mm and capacitors of 15pF, 10pF, 5pF, 2.5pF and 1pF were simulated. As with the number of rungs these values were chosen to represent a practical range for these parameters. The series of values allows trends to be easily discerned from the results. Although the value of 1pF for capacitance could be difficult to achieve in practice when stray capacitance is taken into account, this value was included to approximate the self resonant frequency of each coil.

3. Results

Figure 2 shows the resulting dominant mode resonant frequency when the wire radius and lumped capacitance are varied as mentioned above.

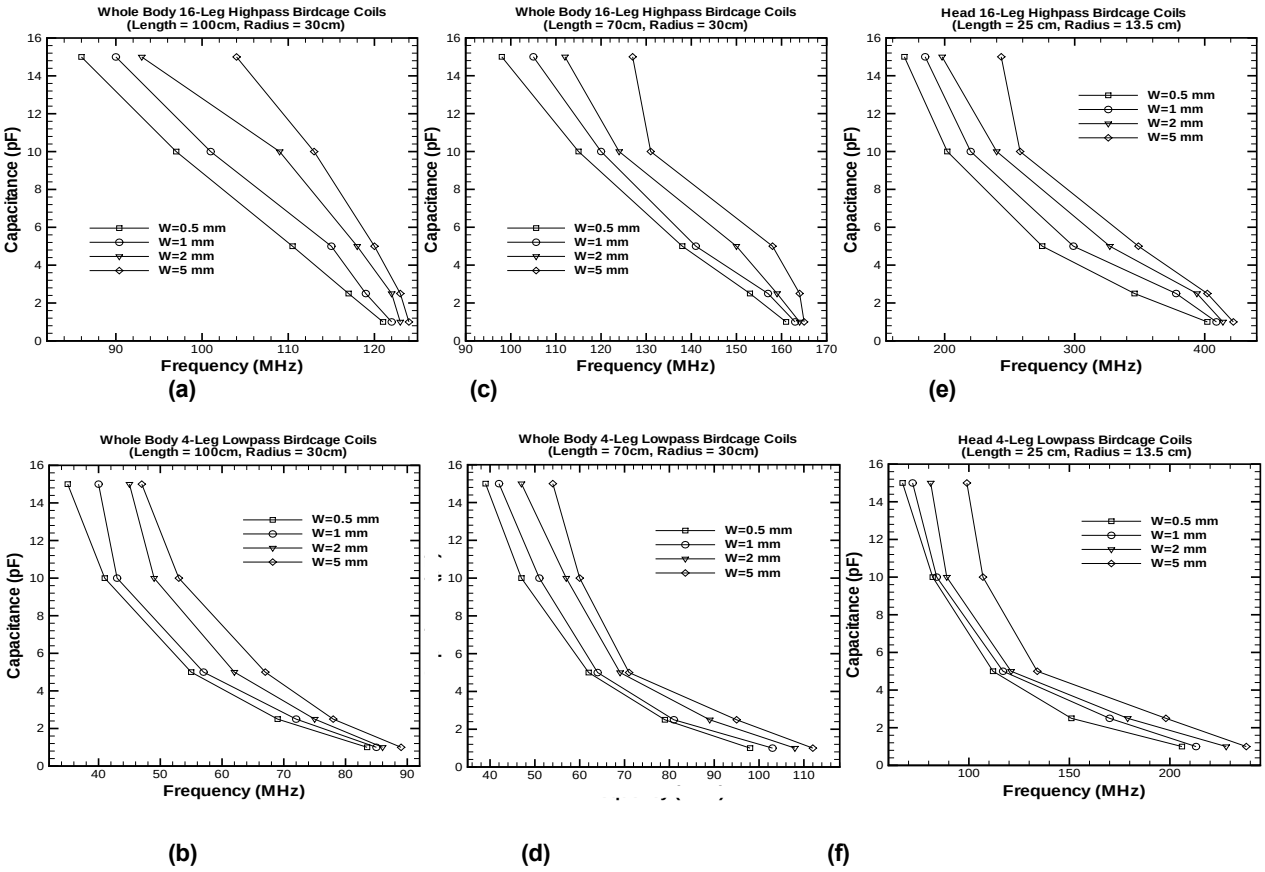

Figure 2 The resonant frequencies for six different coils.
(a) large, high pass (16 rung) body coil (b) large, low pass (4 rung) body coil
(c) small, high pass (16 rung) body coil (d) small, low pass (4 rung) body coil
(e) high pass (16 rung) head coil (f) low pass (4 rung) head coil

Knowing that the current on the rungs should be distributed sinsusoidally, the currents were plotted to give an indication of how the distribution changed with frequency. Figure 3 shows the current distribution on the rungs of the large, high pass, 16 rung body coil at three different frequencies. As there are 11 segments on each of the 16 rungs the x axis range is from 1 to 176.

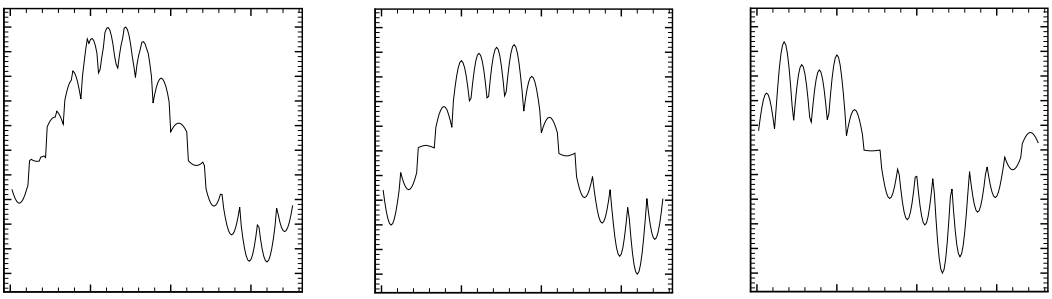

Figure 3. Current distribution on the rungs of the large, high pass, 16-leg Whole body coil
(a) 86 MHz; (b) 104 MHz; (c) 124 MHz

The B1 magnetic field homogeneity was investigated by plotting the magnitude of this field across a section through the centre of the coil. Figure 4 shows the current distribution and field profile for the 16 rung, high pass head coil at three different frequencies.

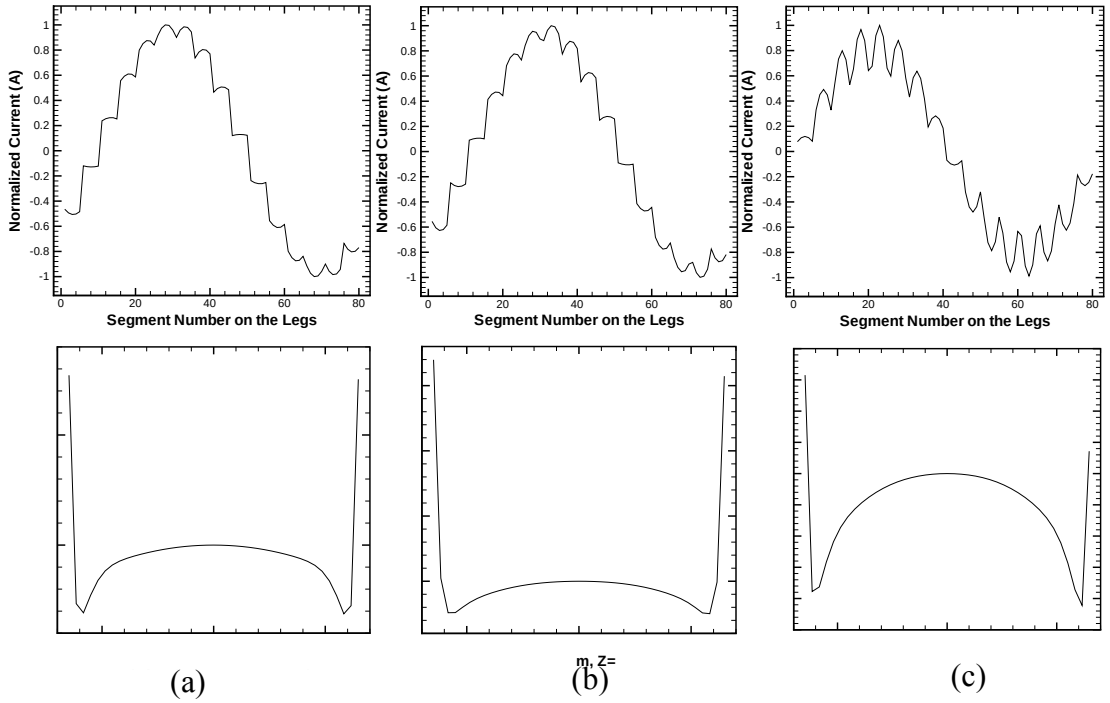

Figure 4 Current distributions (top) and the corresponding B1 field (bottom) for 16-rung, high pass head coil. (a) 169 MHz (b) 275 MHz (c) 402 MHz

4. Discussion and Conclusion

Frequency limits for empty coils

Figure 2 indicates the following approximate self resonant frequencies for the six coils that were simulated:

large, high pass (16 rung) body coil	124 MHz
small, high pass (16 rung) body coil	165 MHz
high pass (16 rung) head coil	422 MHz
large, low pass (4 rung) body coil	89 MHz
small, low pass (4 rung) body coil	112 MHz
low pass (4 rung) head coil	238 MHz

The resonant frequency increased with decreasing capacity and increasing wire radius (decreasing inductance) as expected. From these results it can be seen that the resonant frequency is inversely proportional to the size of the coil. For coils of the same size it demonstrates that the low pass configuration has a lower resonant frequency than the high pass configuration.

Current distributions on the rungs

The plots of current distribution on the segments shows that there is significant departure from the ideal of current that is constant along the length of each rung but varies sinusoidally around the coil even at frequencies well below the maximum. This indicates that the practical limits will be less than those given above as the field will also vary along the axis of the coil and the useful, homogeneous region will be reduced. As shown in Figure 4 the field also varies across the coil at the higher frequencies and reduces the useable volume even further. For these reasons practical limits of approximately half the above values for simulated self resonance will probably be more appropriate when selecting birdcage coils for high field use.

Sample interactions

While only unloaded coils have been considered in these simulations it is known that the introduction of a practical sample with high relative permittivity, conductivity and asymmetry will cause further problems. Even when using TEM or Recav coils with excellent unloaded field distributions, large variations in intensity appear in both experimental and simulated images with

bright spots in the centre at very high fields and frequencies (11.7 T, 470 MHz.). From Figure 5, it can be seen that the homogeneity of the loaded volume coil is getting worse as the frequencies goes higher. In addition, we have also conducted some simulation work on these sample/field interactions and obtained similar conclusion [10]. Therefore, the loading effect is another factor to be taken into account when assessing the upper frequency limit of a particular coil design.

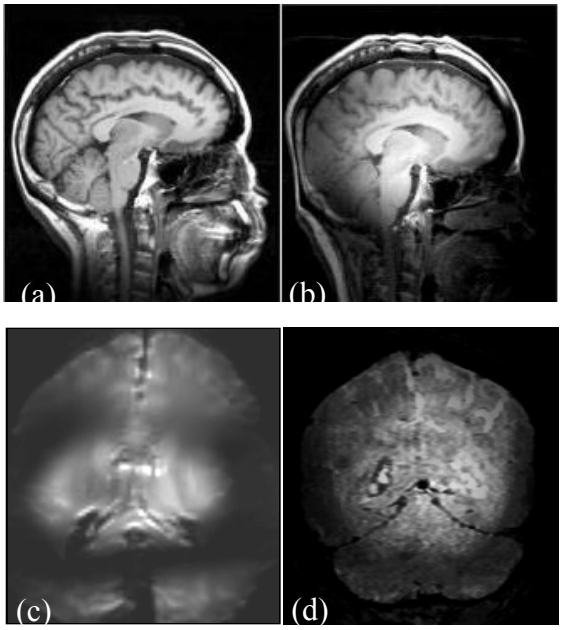

Figure 5
(a) Experimental head image in a TEM coil at 4 T [11];
(b) Experimental head image in a TEM coil at 7 T[11];
(c) Experimental had image in a Recav coil at 11.7 T[10];
(d) Simulated head image in a Recav coil at 11.7 T [10].

References

[1] C.E. Hayse, W.A. Edelstein, J.F. Schenck, O.M. Mueller, M. Eash, An Efficient Highly Homogeneous Radiofrequency Coil for Whole-Body NMR Imaging at 1.5T, J. Magn. Reson. 63: 622-628, (1985).

[2] J.M. Jin, Electromagnetic design and analysis in magnetic resonance imaging, Boca Raton, FL: CRC, (1999).

[3] C. Chin, S. Li, C.M .Collins and M. B. Smith, Mutual inductance Calculation between Ending-Ring Segments for Elliptical Birdcage Coils, ISMRM 5th Scientific Meeting,Vancouver, (1997)

[4] D.I. Hoult, The sensitivity and power deposition of the high field imaging experiment, J Magn. Reson. Imag., 12: 46-67, (2000).

[5] J.T. Vaughan, H.P. Hetherington, J.O. Out, J.W. Pan, G.M. Pohost, High-frequency volume coils for clinical nuclear magnetic resonance imaging and spectroscopy, Magn. Reson. Med., 32: 206-218, (1994).

[6] E.C Wong , E. Boskamp, and J.S Hyde, A volume optimized quadrature elliptical end-cap birdcage brain coil, 11th Annu. Sci. Mtg .Sco .Magn .Reson.Med., 4015, (2002).

[7] P. Röschmann, "High-frequency coil system for a magnetic resonance imaging apparatus," U.S. Patent 4 746 866, 24, (1988).

[8] J. F. Bridges, Cavity resonator with improved magnetic field uniformity for high frequency operation and reduced dielectric heating in NMR imaging devices, U.S. Patent 4 751 464, June 14, (1988).

[9] B.A., Baertlein, O. Ozbay, T. Ibrahim, R. Lee, Y. Yu; A. Kangarlu; P.-M.L. Robitaille, Theoretical model for an MRI radio frequency resonator**,** IEEE Trans. Biomed. Eng., 47(4): 535-546, (2000).

[10] Feng Liu , Bin Xu, Barbara L. Beck , Stephen Blackband and Stuart Crozier, 11T MRI and Numerical Modelling of the Excised, Fixed Human Head, submitted to IEEE Trans. Med. Imag., (2003)

[11] J.T. Vaughan, M. Garwood, C.M. Collins, W. Liu, L. DelaBarre, G. Adriany, P. Andersen, H. Merkle, R. Goebel, M.B. Smith, K. Ugurbil, "7T vs. 4T: RF power, homogeneity, and signal-to-noise comparison in head images," Magn. Reson. Med., 46: 24-30, (2001).

[12] EM Software & Systems. FEKO User's Manual, South Africa, (2000).